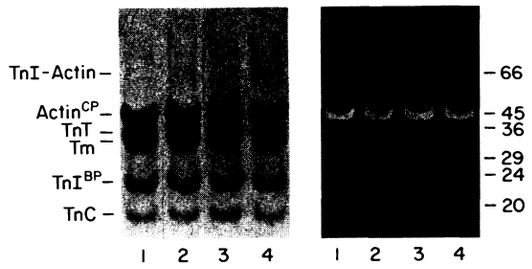

Fig. 2. Polyacrylamide (12.5%) gel electrophoresis showing photo cross-linking between TnI and actin in the reconstituted (TnC-TnI^{BP}-TnT)–Tm–F-actin^{CP} thin filament system in the presence (lanes 1 and 2) or absence (lanes 3 and 4) of Ca^{2+}. (Lanes 1 and 3) Samples before irradiation; (lanes 2 and 4) samples that have been irradiated for 5 min at 4°C. (Left panel) The Coomassie blue–stained gel; (right panel) the fluorescence of the same gel before staining. Labeling of TnI with BP-Mal and of actin with CP-Mal were performed as described in Fig. 1. Samples irradiated (*22*) in the presence of Ca^{2+} contained 0.2 m*M* $CaCl_2$; those irradiated in the absence of Ca^{2+} contained 2 m*M* EGTA and 4 m*M* $MgCl_2$. The positions of molecular mass markers (in kilodaltons) are shown on the right.

modifications on the activity. The regulatory capacity values [defined as $1 - (Act_{Ca^{2+}}/Act_{EGTA})$, where $Act_{Ca^{2+}}$ and Act_{EGTA} are Mg-ATPase activities in the presence and absence of Ca^{2+}, respectively] of (TnC-TnI-TnT)–Tm–F-actin, (TnC-TnI^{DAN}-TnT)–Tm–F-actin^{DAB}, and (TnC-TnI^{BP}-TnT)–Tm–F-actin^{CP} were 0.60, 0.55, and 0.71, respectively (duplicate measurements yielded values of 0.62, 0.61, and 0.65, respectively). Thus, the modifications do not significantly affect the regulatory capacity of the reconstituted thin filaments.

Our energy transfer and photo cross-linking results provide evidence that the protein region containing Cys^{133} of TnI is in close proximity to actin in the absence of Ca^{2+} and moves away from actin in the presence of Ca^{2+}. This movement is most likely induced by the binding of Ca^{2+} to the low-affinity "triggering" sites of TnC, although the possibility of its induction by Ca^{2+} replacing Mg^{2+} at the high-affinity sites cannot be ruled out at present. We have shown that in the ternary Tn complex, the same region of TnI moves toward Cys^{98} of TnC in response to Ca^{2+} (*13*). Thus, the Cys^{133} region of TnI appears to switch between actin and TnC in such a manner that it is close to actin when Ca^{2+} is absent and moves away from actin toward TnC when Ca^{2+} binds to TnC. These results are consistent with the proposed model for Ca^{2+} regulation of striated muscle contraction and confirm the role that TnI plays as a Ca^{2+}-dependent molecular switch in thin filament–based regulation.

Table 2. Parameters of energy transfer between the 1,5-IAEDANS donor and the DAB-Mal acceptor in the reconstituted (TnC-TnI^{DAN}-TnT)–Tm–F-actin^{DAB} thin filament complex as a function of the different metal-binding states. τ_d and τ_{da}, Donor fluorescence lifetimes (in nanoseconds) in the absence and presence of acceptor, respectively; E, transfer efficiency defined as $E = 1 - (\tau_{da}/\tau_d)$; ϕ_d, donor quantum yield; R_o, critical transfer distance obtained under the assumption that $\kappa^2 = 2/3$; R, apparent donor-acceptor separation distance. The lifetimes of (TnC-TnI^{DAN}-TnT)–Tm–F-actin were taken to be τ_d, whereas those of the major component of (TnC-TnI^{DAN}-TnT)–Tm–F-actin^{DAB} were taken to be τ_{da} (Table 1). ϕ_d was calculated as $\phi_d = \phi_d'(\tau_d/\tau_d')$ with values of $\phi_d' = 0.53$ and $\tau_d' = 13.5$ ns, where ϕ_d' and τ_d' are the fluorescence quantum yield and lifetime, respectively, of the 1,5-IAEDANS–labeled αα isoform of Tm (*15*). R_o was calculated as $R_o = R_o'(\tau_d/\tau_d')^{1/6}$, with the value of $R_o' = 39.9$ Å, where R_o' is the critical transfer distance for the 1,5-IAEDANS–DAB-Mal couple attached to ααTm and F-actin, respectively (*15*). R was calculated from the equation $R = R_o(E^{-1} - 1)^{1/6}$.

Metal-binding state	τ_d (ns)	τ_{da} (ns)	E	ϕ_d	R_o (Å)	R (Å)
Ca^{2+}	15.52	13.62	0.122	0.61	40.8	56.7
Mg^{2+}	17.14	8.71	0.492	0.67	41.5	41.7
Apo	17.10	7.15	0.582	0.67	41.5	39.3

REFERENCES AND NOTES

1. S. Ebashi and M. Endo, *Prog. Biophys. Mol. Biol.* **18**, 123 (1968).
2. M. L. Greaser and J. Gergely, *J. Biol. Chem.* **246**, 4226 (1971).
3. S. V. Perry, H. Cole, J. F. Head, F. J. Wilson, *Cold Spring Harbor Symp. Quant. Biol.* **37**, 251 (1972).
4. J. D. Potter and J. Gergely, *Biochemistry* **13**, 2697 (1974).
5. S. E. Hitchcock, *Eur. J. Biochem.* **52**, 255 (1975).
6. Z. Grabarek and J. Gergely, *Acta Biochim. Biophys. Hung.* **22**, 307 (1987).
7. S. S. Margossian and C. Cohen, *J. Mol. Biol.* **81**, 409 (1973).
8. S. E. Hitchcock, H. E. Huxley, A. G. Szent-Györgyi, *ibid.* **80**, 825 (1973).
9. T. Tao, B.-J. Gong, P. C. Leavis, unpublished observations.
10. L. Stryer, *Annu. Rev. Biochem.* **47**, 819 (1978).
11. K. Sutoh and F. Matsuzaki, *Biochemistry* **19**, 3878 (1980).
12. H. D. White, *Methods Enzymol.* **85**, 698 (1982).
13. T. Tao, E. Gowell, G. M. Strasburg, J. Gergely, P. C. Leavis, *Biochemistry* **28**, 5902 (1989).
14. E. W. Small and I. Isenberg, *Biopolymers* **15**, 1093 (1976).
15. T. Tao, M. L. Lamkin, S. S. Lehrer, *Biochemistry* **22**, 3059 (1983).
16. M. L. Greaser and J. Gergely, *J. Biol. Chem.* **248**, 2125 (1973).
17. J. A. Spudich and S. Watt, *ibid.* **246**, 4866 (1971).
18. A. G. Weeds and B. Pope, *J. Mol. Biol.* **111**, 129 (1977).
19. P. C. S. Chong and R. S. Hodges, *J. Biol. Chem.* **257**, 2549 (1982).
20. G. M. Strasburg, P. C. Leavis, J. Gergely, *ibid.* **260**, 366 (1985).
21. T. Tao and J. Cho, *Biochemistry* **18**, 2759 (1979).
22. T. Tao, M. Lamkin, C. J. Scheiner, *Arch. Biochem. Biophys.* **240**, 627 (1985).

23. We thank J. Gergely and Z. Grabarek for advice and discussions. Supported by NIH grants to T. Tao (AR21673) and P. C. Leavis (HL20464) and by the Muscular Dystrophy Association.

24 October 1989; accepted 24 January 1990

Hypoxic Dilation of Coronary Arteries Is Mediated by ATP-Sensitive Potassium Channels

JÜRGEN DAUT, WILLIBALD MAIER-RUDOLPH, NIKOLAS VON BECKERATH, GERHARD MEHRKE, KERSTIN GÜNTHER, LISELOTTE GOEDEL-MEINEN

The function of the heart depends critically on an adequate oxygen supply through the coronary arteries. Coronary arteries dilate when the intravascular oxygen tension decreases. Hypoxic vasodilation in isolated, perfused guinea pig hearts can be prevented by glibenclamide, a blocker of adenosine triphosphate (ATP)–sensitive potassium channels, and can be mimicked by cromakalim, which opens ATP-sensitive potassium channels. Opening of potassium channels in coronary smooth muscle cells and the subsequent drop in intracellular calcium is probably the major cause of hypoxic and ischemic vasodilation in the mammalian heart.

BLOOD FLOW THROUGH THE CORONARY arteries is precisely regulated, and any imbalance between the oxygen supply and the oxygen demand of the heart leads to angina pectoris or to heart failure. A decrease of the oxygen tension in coronary arteries (hypoxia) or an interruption of blood flow (ischemia) causes a marked reduction of the resistance of coronary arteries. The proposed mechanisms underlying this dilation of coronary arteries

J. Daut, N. von Beckerath, G. Mehrke, K. Günther, Physiologisches Institut der Technischen Universität München, Biedersteiner Strasse 29, D-8000 München 40, Federal Republic of Germany.
W. Maier-Rudolph and L. Goedel-Meinen, 1. Medizinische Klinik, Klinikum rechts der Isar der Technischen Universität München, D-8000 München 80, Federal Republic of Germany.

have been controversial. It has been suggested that the hypoxic and ischemic increase in coronary flow may be caused by (i) release from cardiomyocytes of vasodilatory metabolites (*1*) that act on vascular smooth muscle cells (*1, 2*) or on endothelial cells (*3*); (ii) direct effects of intravascular oxygen tension (P_{O_2}) on coronary endothelium that induce release of vasodilatory substances, for example, prostaglandins (*4*) or endothelium-derived relaxing factor (EDRF) (*5*); (iii) direct effects of P_{O_2} on vascular smooth muscle cells (*6*); or (iv) various other mechanisms (*2*).

Our study of hypoxic and ischemic vasodilation was carried out on isolated guinea pig hearts perfused at a constant rate (*7*). The resistance of the coronary arteries was monitored by measuring coronary perfusion pressure (CPP) in the aorta. In addition, the left ventricular pressure (LVP) produced by isovolumetric contractions was measured with a latex balloon inserted into the left ventricle through the pulmonary vein. During hypoxia, there was a decrease in coronary perfusion pressure, indicating a marked vasodilation within 30 s (Fig. 1A). After a 15- or 30-s period of ischemia, a transient vasodilation of nearly the same amplitude as during hypoxia was observed.

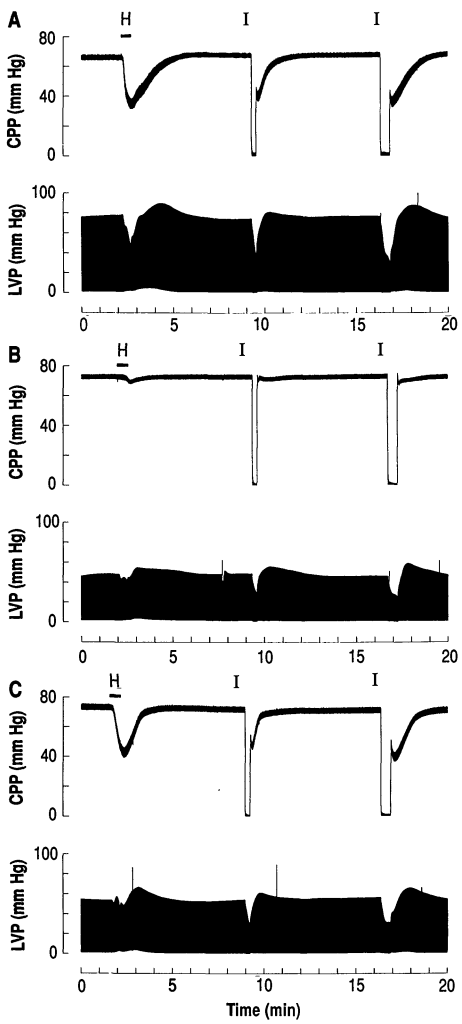

Fig. 1. Effects of hypoxia (H) and ischemia (I) on CPP and LVP. (**A**) Control, (**B**) with 2 μ*M* glibenclamide, and (**C**) 1 hour after removal of glibenclamide.

Smooth muscle cells isolated from mesenteric arteries possess ATP-sensitive K^+ channels (K^+_{ATP} channels) (*8*), which are inhibited by intracellular ATP. Glibenclamide and other antidiabetic sulfonylureas reduce the open probability of K^+_{ATP} channels in various tissues (*8–10*). Both hypoxic vasodilation and ischemic vasodilation were prevented by 2 μ*M* glibenclamide (Fig. 1B, $n = 11$ hearts). Glibenclamide also had a negative inotropic effect of 5 to 20%; the mechanism underlying this effect is still unclear. The effects of glibenclamide on CPP were completely reversible after 1 hour of washing (Fig. 1C), whereas LVP did not always recover completely.

Glibenclamide appears to selectively block K^+_{ATP} channels. No other type of K^+ channel was found to be affected by antidiabetic sulfonylureas (*8, 10, 11*). Thus the results in Fig. 1 are consistent with the idea that early hypoxic vasodilation and ischemic vasodilation may be related to the opening of K^+_{ATP} channels. However, the interpretation of measurements on beating hearts is complicated by the interaction between ventricular pressure and coronary flow. Inotropic or chronotropic effects are usually associated with a change in coronary resistance. Therefore most of our subsequent experiments were carried out in hearts that were arrested with a solution containing 15 m*M* K^+. The maximal vasodilation induced by hypoxia, ischemia, or other interventions in arrested hearts ($n = 36$) was similar to that found in beating hearts.

To determine if coronary endothelial cells participated in the effects described above, we induced vasodilation by three different interventions (Fig. 2): (i) hypoxia, (ii) application of cromakalim (BRL 34915), an antihypertensive drug that opens K^+_{ATP} channels (*8, 10*), and (iii) application of the nonapeptide bradykinin, the action of which is mediated by the endothelium (*12*). The effects of hypoxia and cromakalim were blocked by glibenclamide (Fig. 2), whereas the vasodilation induced by bradykinin was unchanged ($n = 6$). These findings suggest that early hypoxic and ischemic vasodilation are not related to release of EDRF or prostaglandins from the endothelium.

The simplest explanation for our results is that hypoxic and ischemic vasodilation are mediated by opening of K^+_{ATP} channels in coronary smooth muscle cells. However, it could still be argued that it is the decrease of

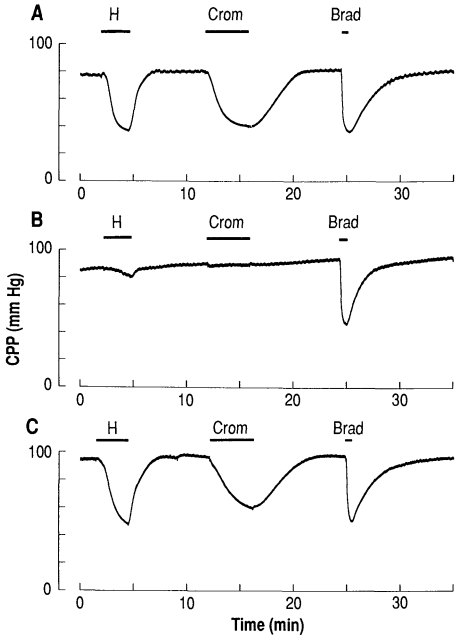

Fig. 2. Effects of hypoxia (H), 200 n*M* cromakalim (Crom) and 500 p*M* bradykinin (Brad) on CPP in the arrested heart. (**A**) Control, (**B**) with 2 μ*M* glibenclamide, and (**C**) 1 hour after removal of glibenclamide.

P_{O_2} per se, or some other oxygen-sensitive mechanism, and not the fall in intracellular ATP, that causes the vasodilation (*5*). Therefore we tried to lower the intracellular ATP concentration in the presence of a high intravascular P_{O_2} by applying the mitochondrial uncoupler 2,4-dinitrophenol (DNP) (Fig. 3A). Perfusion of the heart with 25 μ*M* DNP caused a decrease in coronary perfusion pressure that was similar to that produced by hypoxia. This vasodilation was almost completely blocked by glibenclamide ($n = 4$). Inhibition of oxidative phosphorylation by 200 μ*M* cyanide caused a similar vasodilation, which was also blocked by 2 μ*M* glibenclamide ($n = 3$) (*13*).

These experiments show that substances that decrease intracellular ATP concentration produce a pronounced vasodilation in the presence of a high P_{O_2}. Thus we consider it unlikely that the decrease in coronary resistance during hypoxia is caused directly by the reduction of P_{O_2}. We suggest that early hypoxic and ischemic vasodilation in isolated, perfused guinea pig heart may be mediated by the following sequence of events: (i) Hypoxia and ischemia induce opening of K^+_{ATP} channels in coronary smooth muscle cells; this opening may be mediated by a fall in the intracellular ATP concentration or by a rise in the intracellular adenosine diphosphate concentration (*14*). (ii) The outward current flowing through the K^+_{ATP} channels produces a hyperpolarization. (iii) The hyperpolarization reduces the open probability of voltage-dependent

Ca^{2+} channels (*14*). (iv) This leads to a decrease in intracellular free Ca^{2+} of the smooth muscle cells and thus to a dilation of coronary resistance vessels.

As a test of this hypothesis, we tried to change the membrane potential by an approach that does not involve K^+ channels. Blockage of the electrogenic sodium pump of coronary smooth muscle cells by the fast-acting cardiac glycoside dihydroouabain (DHO) should produce a cell membrane depolarization (*15*) and thus an increase in vascular tone. Addition of 200 μ*M* DHO to the perfusate of the arrested heart caused a rapid increase of coronary perfusion pressure; this effect could be reversed within 2 to 3 min (Fig. 3B). The average increase in CPP produced by 200 μ*M* DHO was 15 mm Hg (n = 5). The increase in CPP within 20 s is primarily due to the depolarization caused by inhibition of the electrogenic pump current. The resulting change in intracellular Na^+ is probably much slower and can be separated kinetically (*16*). When DHO was applied for more than 1 min, a transient decrease in CPP below control values was found after removal of DHO (Fig. 3B). This decrease was probably caused by intracellular Na^+ accumulation during prolonged inhibition of the sodium pump. A rise in intracellular Na^+ stimulates the sodium pump and is expected to produce a transient hyperpolarization of smooth muscle cells after removal of DHO, as has been observed in cardiac ventricular muscle (*16*). Thus both hyperpolarization and depolarization of vascular smooth muscle cells appear to be correlated with changes in coronary resistance.

Can our results be reconciled with the classical hypothesis that hypoxic dilation of coronary arteries may be caused by release of adenosine from cardiomyocytes into the interstitial space (*1, 2*)? Intravascular application of 1 μ*M* adenosine produced a decrease in CPP similar to that observed during hypoxia (Fig. 3C). This effect was reduced to 32 ± 4% (mean ± SEM, n = 5) in the presence of 2 μ*M* glibenclamide (Fig. 3C). These findings might be explained by the hypothesis that adenosine causes the opening of the K^+_{ATP} channels in smooth muscle cells via a receptor-activated G protein–dependent mechanism. The glibenclamide-insensitive component of the action of adenosine may be due to activation of intravascular purinergic receptors on coronary endothelial cells, causing release of EDRF (*17*). Thus we cannot exclude the possibility that release of adenosine from cardiac muscle cells contributes to coronary vasodilation during hypoxia and after ischemia.

Our results suggest that both cromakalim and hypoxia cause relaxation of coronary smooth muscle cells by opening K^+_{ATP} channels. Application of 100 or 500 n*M* cromakalim in the beating heart produced the same degree of vasodilation as hypoxia (Figs. 1A and 3D). The decrease in CPP was accompanied by a small negative inotropic effect (<20%) in the steady state (n = 12), which may be related to a shortening of the ventricular action potential caused by opening of K^+_{ATP} channels in cardiac muscle (*18*). The potency of cromakalim in opening K^+_{ATP} channels and also the potency of glibenclamide in blocking K^+_{ATP} channels varies between cell types and between species (*11*). Several other vasodilating agents such as pinacidil and nicorandil, which are chemically unrelated to cromakalim, also open K^+_{ATP} channels (*8, 19, 20*), but each of the K^+ channel openers has specific effects on regional blood flow (*20, 21*). It may be possible, therefore, to develop K^+ channel–opening drugs that act preferentially on coronary arteries. Such vasodilators might be useful in the therapy of coronary heart disease.

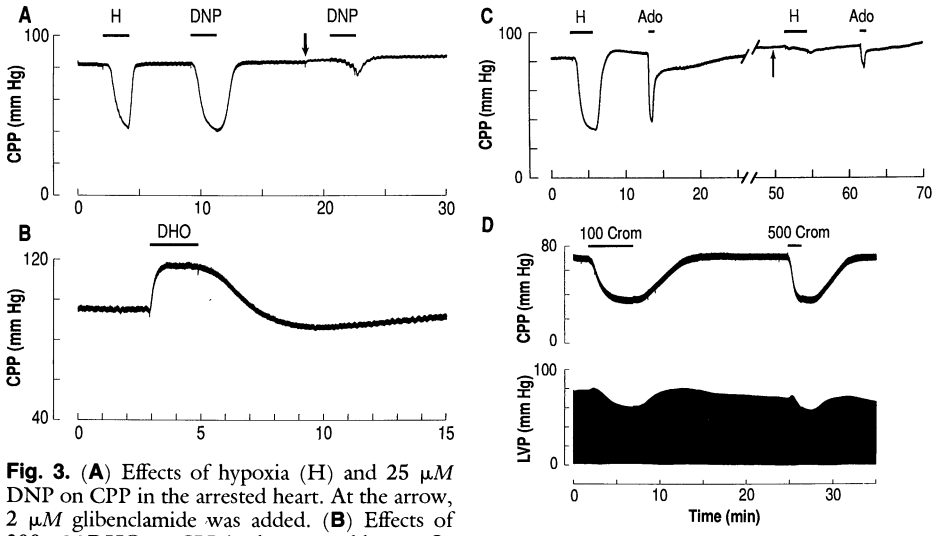

Fig. 3. (**A**) Effects of hypoxia (H) and 25 μ*M* DNP on CPP in the arrested heart. At the arrow, 2 μ*M* glibenclamide was added. (**B**) Effects of 200 μ*M* DHO on CPP in the arrested heart. (**C**) Effects of hypoxia (3 min) and by intravascular application of 1 μ*M* adenosine (Ado) (30 s) on CPP in the arrested heart. At the arrow, 2 μ*M* glibenclamide was added. The effects of glibenclamide in (A) and (C) were fully reversible. (**D**) Effects of 100 and 500 n*M* cromakalim (Crom) on CPP and LVP.

REFERENCES AND NOTES

1. R. M. Berne, *Physiol. Rev.* **44**, 1 (1963); E. Gerlach, B. Deuticke, R. H. Dreisbach, *Naturwissenschaften* **50**, 228 (1963).
2. R. A. Olsson and R. Bünger, *Prog. Cardiovasc. Dis.* **29**, 369 (1987).
3. S. Nees *et al.*, *Basic Res. Cardiol.* **80**, 515 (1985).
4. R. Busse, U. Förstermann, H. Matsuda, U. Pohl, *Pfluegers Arch.* **401**, 77 (1984).
5. U. Pohl and R. Busse, *Am. J. Physiol.* **256**, H1595 (1989).
6. A. E. Chang and R. Detar, *ibid.* **238**, H716 (1980); J. D. Laird, in *Cardiac Metabolism*, A. J. Drake-Holland and M. I. M. Noble, Eds. (Wiley, Chichester, 1983), pp. 257–278.
7. Hearts were rapidly excised from guinea pigs weighing 300 to 400 g, the aorta was cannulated, and the coronary arteries were perfused at a constant rate (4 to 10 ml/min; average, 7 ml/min) by means of a peristaltic pump. Throughout the experiment the heart was immersed in a small, temperature-controlled bath (37°C; volume, 6 ml) with overflow drainage. The perfusion rate was adjusted to give a CPP of 70 to 90 mm Hg. The perfusing solution was warmed to 37°C and contained 116 m*M* NaCl, 5.4 m*M* KCl, 1.8 m*M* $CaCl_2$, 0.8 m*M* $MgCl_2$, 1 m*M* NaH_2PO_4, 24 m*M* $NaHCO_3$, and 10 m*M* glucose; it was equilibrated with 95% O_2 and 5% CO_2 to *p*H 7.4. Hypoxia was induced by switching to an identical solution equilibrated with 95% N_2 and 5% CO_2; the Po_2 in the aorta was <10 mm Hg. To arrest the hearts, KCl was increased to 15 m*M*; this was osmotically compensated for by a reduction of NaCl. The change of solutions was carried out by two inert electric valves (Lee LFYA) mounted between heat exchanger and aortic cannula. Ischemia was induced by opening an outlet immediately above the aorta by means of another electric valve. The spontaneous heart rate was 3.5 to 4 Hz. The hearts were electrically paced at a rate slightly above that. CPP and LVP were recorded by means of two piezoresistive transducers (SensoNor 880). Preload was adjusted to about 0 mm Hg. All records were stored digitally (12 bit; sampling rate, 44 kHz) on a digital audiotape recorder (BioLogic) and transferred to a microcomputer for analysis.
8. N. B. Standen *et al.*, *Science* **245**, 177 (1989).
9. J. De Weille, H. Schmid-Antomarchi, M. Fosset, M. Lazdunski, *Proc. Natl. Acad. Sci. U.S.A.* **85**, 1312 (1988).
10. D. Escande, D. Thuringer, S. Leguern, I. Cavero, *Biochem. Biophys. Res. Commun.* **154**, 620 (1988).
11. F. M. Ashcroft, *Annu. Rev. Neurosci.* **11**, 97 (1988).
12. M. Kelm and J. Schrader, *Eur. J. Pharmacol.* **155**, 317 (1988); R. M. J. Palmer, A. G. Ferrige, S. Moncada, *Nature* **327**, 524 (1987).
13. J. Daut *et al.*, unpublished data.
14. M. J. Dunne, J. A. West-Jordan, R. J. Abraham, R. H. T. Edwards, O. H. Petersen, *J. Membr. Biol.* **104**, 165 (1988).
15. M. T. Nelson, N. B. Standen, J. E. Brayden, J. F. Worley III, *Nature* **336**, 382 (1988).
16. J. Daut, *J. Mol. Cell. Cardiol.* **14**, 189 (1982); ——— and R. Rüdel, *J. Physiol. (London)* **330**, 243 (1982).
17. G. Mehrke and J. Daut, *Pfluegers Arch.* **415** (Suppl. 1), R115 (1990).
18. M. C. Sanguinetti, A. L. Scott, G. J. Zingaro, P. Siegl, *Proc. Natl. Acad. Sci. U.S.A.* **85**, 8360 (1988).
19. N. S. Cook, *Trends Pharmacol. Sci.* **9**, 21 (1988).
20. S. W. Weir and A. H. Weston, *Br. J. Pharmacol.* **88**, 121 (1986).
21. S. D. Longman, J. C. Clapham, C. Wilson, T. C.

Hamilton, *J. Cardiovasc. Pharmacol.* **12**, 535 (1988); T. C. Hamilton and A. H. Weston, *Gen. Pharmacol.* **20**, 1 (1989).

22. We thank F. Altmayr, A. Dischner, L. Müller, and W. Zeitz for technical support, and J. Dudel, W. Baedeker, and H. Blömer for help and advice. Supported by the Deutsche Forschungsgemeinschaft (Da 177/2-4).

27 October 1989; accepted 24 January 1990

Simulation of Paleocortex Performs Hierarchical Clustering

JOSÉ AMBROS-INGERSON, RICHARD GRANGER,* GARY LYNCH

Simulations were performed of layers I and II of olfactory paleocortex, as connected to its primary input structure, olfactory bulb. Induction of synaptic long-term potentiation by means of repetitive sampling of inputs caused the simulation to organize encodings of learned cues into a hierarchical memory that uncovered statistical relationships in the cue environment, corresponding to the performance of hierarchical clustering by the biological network. Simplification led to characterization of those parts of the network responsible for the mechanism, resulting in a novel, efficient algorithm for hierarchical clustering. The hypothesis is put forward that these corticobulbar networks and circuitry of similar design in other brain regions contain computational elements sufficient to construct perceptual hierarchies for use in recognizing environmental cues.

HOW VARIOUS PROPERTIES OF memory might emerge from design features of circuits in cerebral cortex is a major problem area for neural network research (*1, 2*). In previous studies, we addressed this in models of the superficial layers of the olfactory cortex (*3*) by incorporating several of the characteristics of the synaptic long-term potentiation (LTP) effect (*4*). Implementation of a repetitive sampling feature meant to represent the cyclic sniffing behavior of mammals (*5*) produced a system that exhibited a kind of dual encoding of learned cues: early cycles (sniffs) generated response patterns that were common to a subset of cues that resembled each other, whereas later responses were specific to an individual member of the subset. This could mean that the cortical model simply constructs two types of representations (category and individual) or that it discovers hierarchical structure in the cue world and stores memory in this highly structured form. Human subjects in perceptual studies robustly recognize objects first at categorical levels and subsequently at successively subordinate levels (*6*), suggesting the presence of structured memories that are organized and searched hierarchically during recognition. Here we show that the olfactory cortex–olfactory bulb model, during learning, generates a multilevel hierarchical memory that uncovers statistical relationships inherent in collections of learned cues, and, during retrieval, sequentially traverses this hierarchical recognition memory. Moreover, simplification of the network results in an algorithm that provides a novel and efficient solution to the computationally difficult problem of hierarchical clustering.

The elements and circuitry simulated are shown in Fig. 1. Two networks, bulb and cortex, consisting of distinct architectures and physiologies, are extensively connected by both feedforward and feedback projections (*7*). The entire system works in synchrony with a 4- to 7-Hz (theta) sampling pattern that is characteristic of small mammals (*5*). Bulb mitral cells (those neurons innervated by the peripheral receptors and that project to cortex) receive inputs presented repetitively for brief periods. Inputs to the cortical network arise from the resultant synchronous bursting in a subset of mitral cells, yielding cyclic activity in relatively discrete "operation cycles" timelocked to the sampling rhythm. Sparse random connectivity in the simulation selectively activates those cortical cells whose dendrites are most connected to the input lines that are active. Learning increments active synapses on sufficiently depolarized cells via a rule based on LTP (*3*), which has been shown to produce a measurable increment in synaptic strength during even a single 50-ms burst of activity (*4*), that is, within a single operation cycle in the model. Learning requires only a few training trials per

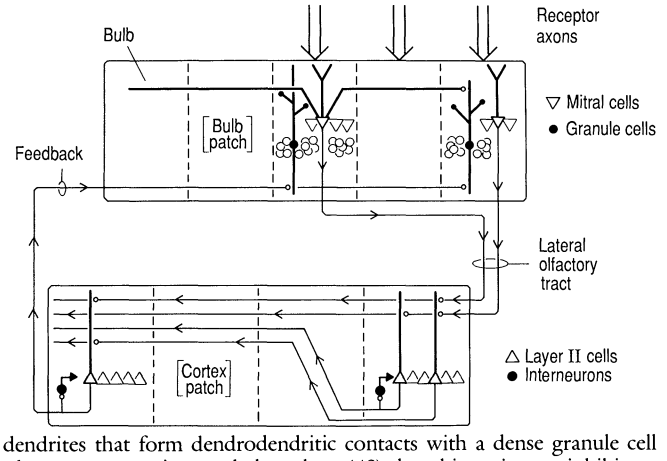

Fig. 1. Anatomical architecture of the bulbar-cortical simulation. The bulb simulation contains 400 projection (mitral) units (simulated neurons), divided into 40 separate groups, each of which receives an input from one group of peripheral receptor axons (*22*). The intensity of an input is reflected in the number of cells within the appropriate group (or groups in the case of multicomponent cues) that it activates. The (excitatory) mitral projection cells in bulb have been shown to have extremely long oblique dendrites that form dendrodendritic contacts with a dense granule cell inhibitory network (*22*). We adopt an assumption made by others (*12*) that this excitatory-inhibitory arrangement serves to normalize the output of the bulb (that is, the total number of mitral cells that are activated is reasonably constant across cues with different intensities and compositions). The inhibitory neurons (granule and probably periglomerular) are represented in the model by a single layer of cells and are innervated by randomly organized excitatory feedback from cortex. The strength of the simulated feedback contacts is set during a "development" period in which hundreds of cues are presented and the strength of feedback synapses allowed to vary according to a correlational (Hebb) rule. The mitral cells of bulb project sparsely and nontropographically to the outermost layer of olfactory cortex via the LOT, both biologically (7) and in the simulation. The cortex is simulated as a layer of 1000 excitatory layer II cells that are assumed in the model to be arranged into patches of 20 cells each by the radial axonal arborizations of local (feedback) inhibitory interneurons. The modeled neurons sum the voltages from their active synaptic inputs and require different amounts of depolarization for discharges, bursts of discharges, and for induction of synaptic change via LTP. A more detailed simulation of individual patches has shown that active cells that trigger inhibitory interneurons can suppress firing by other cells in a patch; because of this, typically only one or two cells in a patch will discharge in response to bulbar inputs, making each patch into a competitive (or modified winners-take-all) arrangement of the type discussed by many authors (*9, 10*). Such an arrangement is assumed in the present simulation. Each cortical cell receives input from the LOT and from a feedforward associational system generated by the cortical neurons themselves, in both cortex (*7, 23*) and the simulation. The operating rules for the model are based on physiological data reported in the literature (*5, 24*).

Center for the Neurobiology of Learning and Memory, University of California, Irvine, CA 92717.

*To whom correspondence should be addressed.